

Type Ia supernovae observations support the hypothesis of a static universe

David. F. Crawford ^{*}

*Astronomical Society of Australia,
Retired from School of Physics, University of Sydney.
44 Market St, Naremburn, 2065, NSW, Australia*

Accepted XXX. Received YYY; in original form ZZZ

ABSTRACT

This paper considers the hypothesis that the universe is static and demonstrates that type Ia supernova observations which appear to provide strong support for time dilation (and thus for an expanding universe) are in agreement with a static universe. An important anomaly is discovered in the standard calibration method which is that the reference template light curves have widths that are proportional to the rest-frame wavelength. The implication is that the observed light-curve widths do not show time dilation. Thus the time-dilation corrections are unwarranted and the universe is static. An important consideration is the Phillips relation, a correlation between the peak luminosity and the width of type Ia supernovae. Using the Phillips relation the analysis of a recent compilation of type Ia supernova observations is re-examined and it is shown that these observations are consistent with a static universe. It is also argued that the photometric redshift relation and spectroscopic ages are consistent with a static universe. As a separate but related issue it is shown that in the static model the density distribution of type Ia supernovae as a function of redshift agrees with the observations. All the evidence shows that the hypothesis of a static universe is supported.

Key words: cosmology:miscellaneous–supernovae:general

1 INTRODUCTION

Modern cosmology is dominated by the Big Bang theory, which attempts to bring together observational astronomy and particle physics. It has been observed that type Ia supernovae are transient phenomena that take about ten days to reach a peak brightness and then the brightness decreases at a slower rate. Type Ia supernovae are also known for their remarkably constant absolute peak magnitudes which make them excellent cosmological probes. Including the light-curve widths using the Phillips relation (a correlation between the peak luminosity and the width of type Ia supernovae) makes a better fiducial constant than just the magnitude.

The standard cosmological model of an expanding universe requires that the widths of the light curves must increase with redshift due to time dilation. The observed Hubble redshift, z , is defined as the ratio of the observed wavelength to the emitted wavelength minus one. In an expansion model the ratio of any observed time period to the emitted time period is identical to the ratio of the wavelengths,

namely $(1 + z)$. This is true for any time interval and is the time dilation. Any challenge to the standard model such as a static model must show that observations of SNe light-curve widths do not have time dilation even though the observed wavelengths show a redshift.

The first strong evidence for time dilation in type Ia supernovae was provided by Leibundgut et al. (1996) with one supernova and Goldhaber et al. (1996) with seven SNe. This was quickly followed by multiple SNe results from Goldhaber (1997); Perlmutter et al. (1999); Goldhaber et al. (2001). These papers record developments in both SNe observations and analysis, the results of which are asserted to provide strong evidence for an expansion model chiefly because they show that the width of type Ia supernova light curves appears to increase with redshift in good agreement (but not completely accurately) with time dilation.

This paper has two major sections. The first section provides the major result that the observations do not show time dilation and the second section extends the analysis to include comparisons of the light-curve widths and peak magnitude between an expanding model and a static model.

Both sections are based on the extensive analysis of type

^{*} E-mail: davdcraw@bigpond.net.au

Ia supernovae (for brevity SNe) observations provided by [Betoule et al. \(2014\)](#) (hereafter B14).

The aim of the first section is to show that the observed light curves of SNe provided by B14 do not show any evidence of time dilation. The argument is based on the discovery of an anomaly in the light-curve calibration process. Note that in effect the calibrated light-curve width is the observed width divided by the width derived from a common reference template. The anomaly is that the template used by B14 produces widths that are, within statistical fluctuations, proportional to the rest-frame (emitted frame) wavelength. In other words the ratio of two template widths is equal to the ratio of the wavelengths. One consequence is that the widths for a filter as a function of redshift exactly mimic time dilation corrections. There are three possible explanations for the anomaly: it shows the intrinsic width of SNe as a function of wavelength, there is an evolution in widths that exactly counters time dilation, or there is no time dilation and it shows the unwarranted time dilation correction.

The second section compares the results for fiducial constants, absolute peak magnitudes and light-curve widths of the B14 SNe for an expansion model and for a static model (curvature cosmology: briefly described in Appendix A). The results for the static model show the fiducial constant, peak magnitude and light-curve width do not have any significant dependence on redshift. It is also possible to explain why the expansion model can also provide good agreement with the data.

There are two further findings from SNe observations that appear to support the expansion model. First is the apparent dependence of photometric-redshift observations on redshift. These are observations that photometric properties of type Ia supernova spectra, as distinct from spectral wavelength measurements used to determine redshift, show a redshift dependence. However what they show is a light-curve width dependence not a redshift dependence. Second the age of a spectrum is the number of days between the observation of the spectrum and the epoch of the peak magnitude of the supernova. The ability to determine the age from subtle changes in the spectrum provides an independent method of estimating the light-curve width of the supernova. Provided it is not interpreted as a redshift dependence this light-curve width dependence is consistent with a static cosmology.

In a separate analysis of density of SNe observations it is shown that the static model can predict the density distribution of the Supernova Legacy Survey (SNLS) SNe as a function of redshift without the need for evolution.

The distance modulus (equation A5) and the volume function (equation A4) for the static model are described in Appendix A. The Big Bang distance-modulus used is for the modified Λ -CDM model (the required equations are provided in Appendix B). For both cosmologies the reduced Hubble constant is $h=0.7$. In order to avoid ambiguity all measurements dependent on the expansion model are denoted by the suffix “B”(Big Bang), whereas all measurements dependent on the static model are denoted by the suffix “S”.

2 THE SNE DATA SET

Recently B14 have provided an update of the [Conley et al. \(2011\)](#) analysis with better optical calibrations and more SNe. This JLA (Joint Light-curve Analysis) list sample has 720 SNe from the Supernova Legacy Survey (SNLS), nearby SNe (lowZ), the Sloan Digital Sky Survey (SDSS) ([Holtzman et al. 2008](#); [Kessler et al. 2009](#)) and those revealed by the Hubble Space Telescope (HST) ([Riess et al. 2007](#)). For each supernova, B14 provide the redshift, z , the apparent B band peak magnitude, m_B , a light-curve stretching parameter, X_1 , and the colour-measure, c_B , all with measurement uncertainty estimates. Since [Conley et al. \(2011\)](#) used a stretch factor that is more intuitive than X_1 the stretch factors, s_B , were determined by equation 1 ([Guy et al. 2007](#))

$$s_B = 0.98 + 0.091X_1 + 0.003X_1^2 - 0.00074X_1^3. \quad (1)$$

In order to simplify the analysis a colour-luminosity correction of $-3.139c_B$ (B14) is added to the apparent-peak magnitudes to get corrected apparent-peak magnitudes. Then to the first order these modified magnitudes are independent of the colour-measure.

3 THE B14 CALIBRATION METHOD

This paper argues that there is a major anomaly in the B14 calibration method in that the template light curve width is proportional to the rest-frame wavelength. As indicated in Figure 1 of [Goobar & Leibundgut \(2011\)](#) and Fig 1 (below) intrinsic SNe light curves can have a wide variation as a function of observed wavelength. The B14 calibration method ([Guy et al. 2007](#)) uses a light-curve template to eliminate the effects of these intrinsic variations from the observed supernova light curves. They assume that the expansion model is correct and therefore divide the epoch differences for each supernova by $(1+z)$ to remove the presumed time dilation and thus change the width to a stretch factor. This correction is made prior to the calibration.

The calibration method has two main components. The first is to obtain the template light curves by averaging the observed light curves as a function of rest-frame wavelength. The second component determines the light curve width for each supernova by getting the best fit between the (usually sparse) flux densities and the template light curve with the peak height and the width being free parameters. In effect the calibrated supernova width is the ratio of the observed width to the template width. Because of the sparse data for most SNe this is a difficult process that must be iterated many times in order to obtain a stable template.

The B14 calibration method uses the SALT2 template which provides the expected flux density of the supernova light curve as a function of both the rest-frame wavelength and the difference between the observed epoch and the epoch of maximum response. The light-curve template file, `Salt2.template_0.dat`, provides the response for 20 days prior to the maximum and 50 days after the maximum for rest-frame wavelengths from 200 nm to 920 nm in steps of 5 nm. The template file and filter files for the JLA analysis were taken from the SNANA ([Kessler et al. 2009](#)) website.

In order to investigate this anomaly a program was written to extract the light curve for any filter and for any red-

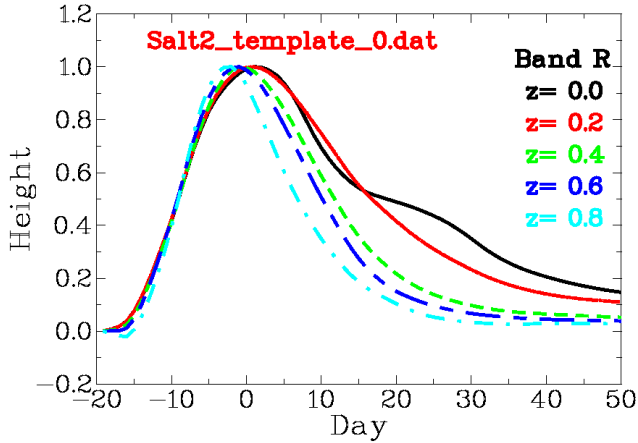


Figure 1. Plot of the template light curve for the R-band at the redshifts of 0, 0.2, 0.4, 0.6 and 0.8. All are normalised to have the same peak value. Clearly the higher redshift curves are narrower than those for lower redshift curves

shift. This procedure not only represents the use of the template but it helps avoid the poorly sampled parts of the template. Fig 1 shows the shape of the light curve derived from the template for the observed R-band at five different redshifts where all curves have been normalized to have the same maximum height. It is apparent that there are variations in shape and width as a function of redshift and the widths are clearly narrower at higher redshifts.

This variation in light-curve width for filter using the standard reference template was investigated further by measuring the distance between the half maximum points on the template light curve for three bands and each with ten redshifts. Fig 2 shows a plot of the reciprocal of these widths (normalized to the value at zero redshift) as a function of redshift. The dashed line is the function $1+z$. For all 36 points the best fitted linear function is $(1.004 \pm 0.041) + (1.071 \pm 0.063)z$. This function is consistent with the template light-curve widths being proportional to the rest-frame wavelength. The anomaly in the B14 calibration method is that such a strong variation of template widths with rest-frame wavelength is unexpected.

If the anomaly is intrinsic then it should be observed in the relative widths between different filter observations for individual supernovae. In the SNANA data there are 45 SNe that have good observations in four or more filters and have observations prior to the maximum. A least squares fit was done between the ratio of the width for each filter to the average width and the ratio of central wavelength for each filter to the average wavelength. The fit for each filter was done with the same reference light curve for each filter and no time dilation correction was applied. The average weighted slope was -0.095 ± 0.116 which is completely incompatible with the expected slope of one. Hence the anomaly can not be an intrinsic property of the SNe.

3.1 Cosmological implications

The template light curve is the average of all the SNe light curves. The presence of cosmological information in the tem-

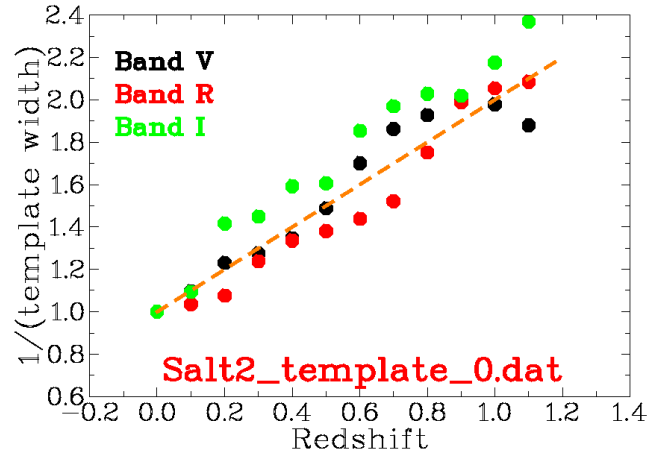


Figure 2. Plot of the reciprocal of the width of the template light curve for the V-band, R-band and I-band as a function of redshift. The straight line is the function $1+z$ and the best fit straight line has a slope 1.071 ± 0.063 . The anomaly in the calibration method is that these data points should be on a horizontal line.

plate depends on the spread of wavelengths observed for each supernova being less than the total spread of rest-frame wavelengths. For the B14 data set the typical wavelength spread is less than half the total spread.

Fig 2 shows that the width of the template light curve, which is the intrinsic light curve in the rest-frame, depends strongly on wavelength so that they mimic the time dilation corrections. Removing the time dilation correction factor, $1/(1+z)$, from the 38 template light-curve widths (used above) shows a dependence of template light curve width on redshift of $1.002 \pm 0.044 - (0.034 \pm 0.037)z$. Since this is an estimate of the observed SNe light-curve widths it shows that they have, as a group, negligible linear variation of width with redshift.

To summarise there are three possible explanations for the calibration anomaly:

- (i) The anomalous light-curve widths are intrinsic. As shown above this is incompatible with the relative widths from different filters for each SNe.
- (ii) There is evolution that exactly counters the result time dilation so that the observed widths do not show any redshift dependence. Since this would be very strong evolution and is not supported by other evidence it is extremely unlikely.
- (iii) There is no time dilation in the observed widths and thus the anomaly in the template light curves comes from the unwarranted application of a time dilation correction. Thus the universe is static.

4 THE PEAK MAGNITUDE AND FIDUCIAL VARIABLES

4.1 The Phillips relation

Phillips (1993) found that the absolute peak luminosities of SNe appear to be tightly correlated with the rate of decline of the B light curve. This correlation may be inter-

preted as being between magnitude and light curve width. The Phillips relation is intrinsic to the SNe and thus independent of any cosmological model. Rather than using peak luminosity and width the more useful variables are peak magnitude and width. In order to simplify later expressions in this paper the width and stretch factors are measured in magnitude units. Define a new variable, W , such that $W = 2.5 \log(w)$ where the width, w , is relative to a standard light curve. Thus the reference value of W is zero. Similarly define the stretch factor measured in magnitudes as $S = 2.5 \log(s) \approx 1.086(s - 1)$ and define a new redshift variable $Z = 2.5 \log(1 + z) \approx 1.086z$ which is the redshift measured in magnitudes. Thus the relationship $w = (1 + z)s$ becomes $W = S + Z$. One advantage of using W is that although W can be unbounded, w is always greater than zero.

The Phillips relation between the apparent peak magnitude, m , and W is defined by the equation $m = m_0 - \alpha W$, where m_0 is the expected apparent peak magnitude and where α is the slope and by convention is positive. This equation corresponds to a luminosity equation: luminosity $\propto w^\alpha$.

In the current notation the use of the Phillips relation at a particular redshift requires that, within statistical fluctuations, $m + \alpha W$ is constant. Hence since $M = m - \mu$, where μ is the distance modulus, then for all redshifts $M + \alpha W$ is constant. Early observations showed that all SNe have about the same magnitude. Then if the cosmology is correct the fiducial constant E defined by

$$E = M + \alpha W \quad (2)$$

is a better fiducial constant than M and can be used for cosmological investigations.

B14 provide a value for α that allowing for equation 1 is $\alpha = 1.42 \pm 0.08$. Conley et al. (2011) suggest $\alpha = 1.37$ whereas Sullivan et al. (2011) have values near 1.39. Since the main aim of this paper is to compare cosmological models the important aspect is to compare SNe characteristics between low and high redshifts. Thus the best estimate of α is obtained by minimizing the χ^2 if the fit of equation 2 to a constant for nearby SNe. Furthermore any distinction between widths and stretch factors is removed by subtracting a linear fit relative to redshift from the absolute peak magnitudes and the widths before the minimization process. The minimization with respect to S_B using the 118 “lowZ” SNe produces the value $\alpha = 1.36 \pm 0.16$ which agrees with the B14 value. Thus $\alpha = 1.36$ is used throughout this paper.

4.2 Expansion model

Although the literature on the analysis of SNe in an expansion model is comprehensive and extensive (Goobar & Leibundgut 2011), the following reanalysis provides a brief summary of results for later comparison with those from a static model. There are two reasons for this reanalysis, first to put them in the same form as the later results and second to provide results using S_B (the stretch factor measured in magnitudes). Since $W = S + Z$ any intrinsic variation in W_B has the same variation in S_B . The estimate of the fiducial constant E_B is the absolute magnitude corrected for the Phillips relation and for any type Ia supernova with appar-

Table 1. Regressions: verses redshift, z

Row	Var.	Offset	Slope	Res.
1	s_B	0.953 ± 0.004	0.099 ± 0.017	0.080
2	S_B	-0.041 ± 0.006	0.102 ± 0.018	0.089
3	W_B	0.005 ± 0.006	0.818 ± 0.013	0.096
4	c_B	-0.005 ± 0.004	-0.056 ± 0.014	0.079
5	M_B	-19.086 ± 0.010	-0.121 ± 0.027	0.200
6	E_B	-19.133 ± 0.010	-0.042 ± 0.023	0.165
7	W_S	-0.041 ± 0.004	0.102 ± 0.018	0.089
8	M_S	-19.054 ± 0.012	-0.014 ± 0.027	0.196
9	E_S	-19.101 ± 0.010	0.069 ± 0.023	0.165

ent magnitude, m_B , it is

$$E_B = M_B + \alpha S_B = m_B - \mu_B + \alpha S_B, \quad (3)$$

where $M_B = m_B - \mu_B$ is the absolute magnitude for an expansion cosmology and μ_B (equation B2) is the distance modulus. It is E_B that is an estimate of the fiducial constant deemed to be constant for all SNe. Since at any redshift the expected value of the stretch factor, S , is zero then the expected value of M_B is M_0 .

Table 1 shows results for important regressions as a function of redshift (z) for both cosmological models which were obtained using the B14 results. In all rows the regressions were for the complete 740 SNe and the residuals (in magnitudes) are the residuals after the linear fit. The regression allowed for uncertainties in both variables and the uncertainties in the offset and slope were multiplied by the square root of the ratio of the $\chi^2/(N - 2)$ where N is the number of paired values. That is the original uncertainties were used only to produce weight factors and the final uncertainties reflect internal consistency.

Row 1 shows the regression for the stretch factor, s_B . Row 2 shows the regression for the stretch factor, $S_B = 2.5 \log(s_B)$. Row 3 shows the regression for the width, $W_B = 2.5 \log(w_B)$. Row 4 shows the regression for the colour-measure, c_B . Row 5 shows the regression for the magnitude, M_B . Row 6 shows the regression for the fiducial constant, E_B .

Row 6 shows that E_B , with its insignificant slope and small variance, is a good fiducial constant that agrees with the B14 fiducial constant E_B^\dagger . Furthermore the colour-measure (row 4) has a significant redshift dependence.

Both M_B and S_B have small but significant redshift dependencies. Since the stretch factor of SNe is intrinsic it should not have any dependence on redshift. This dependency is the major factor that has led to the idea of an acceleration of the universe and the concept of dark energy. However the property of the calibration method (section 3) means that this significant redshift dependence is probably an artefact and the results do not show strong support for the expansion model. At best they show consistency with the expansion model.

Some results, obtained later (section 4.3), from the static cosmological model are also shown in Table 1, in which row 7 shows the regression for the static model width, W_S , row 8 shows the regression for the absolute magnitude, M_S , and row 9 shows the regression for the fiducial constant, E_S .

4.3 Static model

A fundamental requirement of a static model is that there is no time dilation and thus the Hubble redshift is due to some mechanism other than universal expansion. For the B14 data and calibration method the difference between the expansion model and the static model is in the interpretation of calibrated parameters. The expansion model has apparent peak magnitude and stretch factors and the static model has apparent peak magnitude and widths.

The Phillips relation for a static model and for any type Ia supernova is

$$E_S = M_S + \alpha W_S = m_S - \mu_S + \alpha W_S, \quad (4)$$

where $M_S = m_S - \mu_S$ is the observed absolute peak magnitude, m_S is the apparent peak magnitude, and the static cosmology distance modulus is μ_S (equation A5). For a static model and for all redshifts the expected value of W_S is zero and the expected value for E_S and M_S is M_0 .

Consider the expected peak magnitude and widths for SNe at a fixed redshift. Then because the Phillips relation is an intrinsic property of SNe the expected values must satisfy

$$m_S + \alpha W_S = m_B + \alpha W_B = m_B + \alpha(S_B - Z) \quad (5)$$

We can choose any value for m_S and W_S provided that equation 5 is satisfied. The obvious choice that satisfies the requirement that in the static model the widths must be constant is to put W_S equal to the stretch factor which produces

$$m_S = m_B - \alpha Z \text{ and } W_S = S_B. \quad (6)$$

These equations show that the expected value for the peak magnitude for the static model, m_S , is significantly brighter than that for the expansion model. Note that m_B and m_S are both apparent magnitudes in the sense that no distance modulus is involved but not in the sense that they apply to a single observation.

Because of the calibration method the static widths are identical to the expansion stretch parameters. Fig 3 shows a scatter plot of the static model widths, W_S , as a function of redshift. The regression equation for this width is shown in row 7 of Table 1 and it shows that they have a small but significant redshift dependence. As previously argued (section 3) the erroneous application of the time dilation correction will to the first order be removed by the B14 analysis. The small redshift dependence may be due to second order effects. Without a complete re-analysis without this erroneous correction we can conclude only that the light-curve widths are consistent with the static model. The prediction is that if the universe is static a re-analysis will not show any significant redshift dependence in the calibrated widths.

Figure 4 shows a plot of the static model absolute magnitude, M_S , as a function of redshift. The regression results are shown in row 8 of Table 1 and show that M_S has a small but just significant (5.2σ) redshift dependence. Note that whereas the expansion model distance modulus has, over the years, been fine-tuned to produce a good fiducial constant the static model distance modulus was derived completely independently of supernova observations and has no free parameters.

Figure 5 shows a plot of the static model fiducial constant, E_S , as a function of redshift. The regression results are

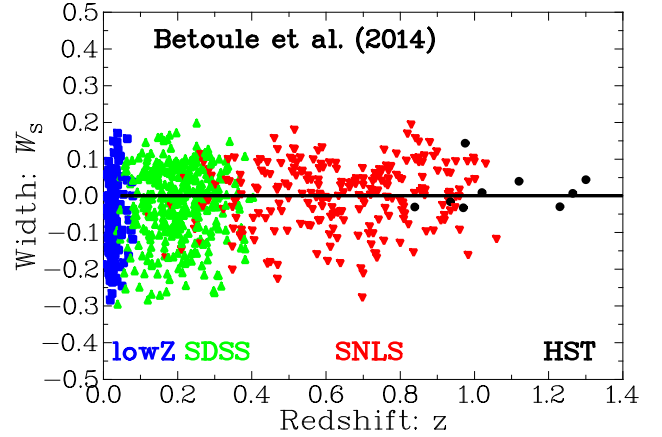


Figure 3. Scatter plot of static model width, W_S , as a function of redshift, z . The solid (black) line shows the zero axis

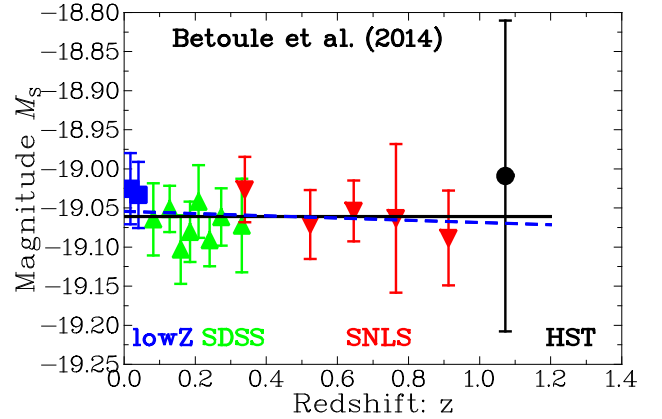


Figure 4. Observed static model absolute peak magnitude, M_S as a function of redshift, z . The dashed (blue) line shows the regression equation $-19.054 - 0.014z$. The solid (black) line is the best fit constant value at -19.054 mag.

shown in row 9 of Table 1 and show that E_S has a negligible redshift dependence.

It is of interest to see why both the expansion model and the static model can be compatible with the data. Consider the relationship between the two absolute magnitudes, namely

$$M_S = M_B + \mu_B - \mu_S - \alpha Z = M_B + f(z) \quad (7)$$

where $f(z)$ is defined by

$$f(z) = \mu_B - \mu_S - \alpha Z. \quad (8)$$

What is remarkable is that $f(z)$ is close to zero over the redshift range of the B14 SNe. The function $f(z)$ starts at zero and has a maximum of ≈ 0.1 mag at $z = 0.8$ and falling to 0.07 mag at $z = 1.3$.

These figures and regressions show that for B14 data the widths, absolute peak magnitudes and fiducial constants of SNe are consistent with a static universe.

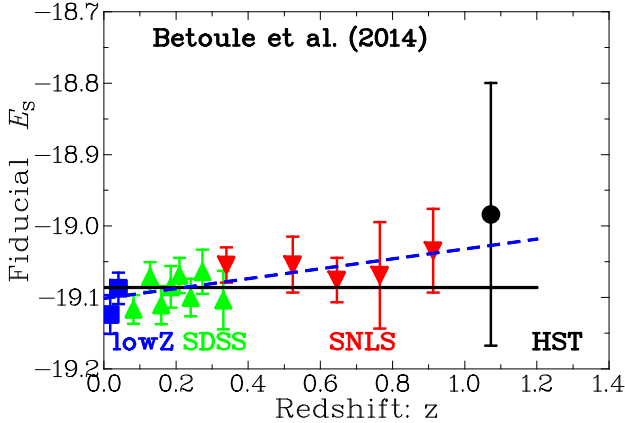


Figure 5. Plot of the static model fiducial constant, E_s as a function of redshift, z . The dashed (blue) line shows the regression equation $-19.101 + 0.069z$. The solid (black) line is the best fit constant value at -19.101 mag.

4.4 Apparent extra wide SNe

There are reports of SNe with very wide light curves that are inconsistent with a static model. An example of apparent extra wide light curves is the 14 light curves shown by Suzuki et al. (2012). For these supernovae the redshifts vary from 0.623 to 1.415 and the light curve (expansion model) widths vary from 1.48 to 2.43. These SNe were analysed using SALT2 which because of the property described in section 3 means that the static model widths are equal to the stretch factors which vary from 0.77 to 1.09. Thus these static model widths are well within the expected range. The apparent extra wide SNe are a consequence of using the wrong paradigm.

However there is a selection effect on the width that can be important. B14 require that $-3 < X_1 < 3$ and Conley et al. (2011) require that the stretch factor is in the equivalent range ($0.7 < s < 1.3$). Since resources are limited the search for high redshift SNe requires that the selection criteria are applied early in the search procedure. Typically this done by applying limits on the rest-frame rise and fall times. If this selection is done independently of the calibration method then it will tend to select SNe that have a static model width near $(1+z)$. Furthermore any bias in favour of brighter supernovae will, because of the Phillips relationship, produce a bias towards wider supernovae. Consequently a bias towards wider light curves at larger redshifts is expected.

4.5 Other redshift evidence

Clearly the redshift of a SNe could be estimated by comparing its wavelength spectrum to the average rest-frame wavelength dependence. For example ever since Tripp (1998) showed that there was a correlation between redshifts of SNe and their colour index B-V there has been a considerable effort (Howell et al. 2007; Bazin et al. 2011; Guy et al. 2007; Mohlabeng & Ralston 2013; Wang & Wang 2013) to use this correlation in order to develop a predictor of the redshift from photometric measurements. However in a static

universe although this is a valid estimate of the light-curve widths it is not evidence for time dilation. It is only in the expansion model that the redshift is related to time dilation and therefore with light-curve width.

Another example is spectroscopic ages. SNe show a consistent variation in characteristics of their spectra with the number of days before and after the maximum. This variation is due to changes in composition, changes in the velocity of the ejecta and the depth of penetration of the ejecta. Blondin et al. (2008) have made a comprehensive analysis of these spectra for both local SNe and 13 high redshift SNe that shows that the age (the position in the light curve from the position of the peak luminosity) of a spectrum can be estimated to within 1-3 days. If there are two or more spectra the aging rate and therefore the width can be estimated. In their analysis they explicitly assumed that this width dependence was a measure of redshift which is true only for the expansion model.

4.6 Density of SNLS SNe

The SNLS and the SDSS surveys both use the technique of *wide-field rolling survey* in which the same section of the sky is repeatedly observed in a regular manner. Whenever there is sudden brightening a possible supernova is flagged. The magnitude at this position is repeatedly measured and, if it passes selection criteria, a spectrum is taken and the redshift is measured. The important aspect of this technique is that to the first order and within the selected magnitude range there is no selection on redshift. Thus in a static model the relative number of SNe that are observed as a function of redshift depends only on the differential volume at that redshift. Different surveys have different time coverage and cover quite different areas. Therefore this analysis must be applied separately to each survey. Here the analysis is limited to the SNLS survey since it covered the largest redshift range.

Assuming that the density of supernova type Ia progenitors and their production rate for a particular survey is independent of redshift, the number expected in a survey is proportional to the density times the observed volume (equation A4, below). We assume that the only selection criterion is that the observed SNe have an apparent magnitude greater than $m_s = 26 - \alpha Z$ mag (equation 4) and that the magnitude distribution is Gaussian with a standard deviation of 0.2 mag.

The number of observed SNe in the SNLS survey are plotted as a function of redshift in Fig 6. The solid (red) line shows the expected distribution for a static model with SNe selected by apparent expansion model magnitude. For comparison the results for the expansion model assuming that the magnitudes have the same Gaussian distribution and magnitude cut off of 26 mag is shown as the dashed (blue) line.

In both models the density was chosen to match the observed counts by using a χ^2 fit for the first six points (with count ≥ 5 and with $z < 0.75$) where the selection process has negligible effect. The multiplier for equation (A4) with a range of ± 0.05 about each z value was 3.04 kpc^{-3} . The important point is that the position of the turn over near $z = 0.7$ for the static model is in reasonable agreement with the observations. Whereas the turn over for the expansion

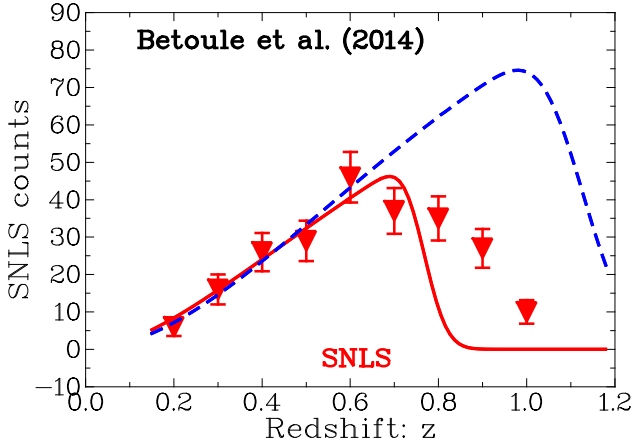


Figure 6. Plot of the observed number of SNe for the SNLS survey as a function of redshift, z . The solid (red) line is the expected number distribution for a static model with an apparent magnitude cut off of $26 - \alpha_Z$ mag. The dashed (blue) line is the expected distribution for an expansion model with an apparent magnitude cut off of 26 mag.

model is at larger redshifts. In the expansion model this discrepancy is explained by evolution.

5 DISCUSSION

Due to an anomaly in the calibration method the B14 template shows a wavelength dependence of light-curve widths that implies that the time dilation corrections are unwarranted. Thus the observed observations do not show any time dilation effects. This is strong support for a static universe.

From the analysis of the B14 SNe data the main difference between the two cosmologies is in the composition of the fiducial constants. The expansion model decomposes the fiducial constant into a magnitude and stretch factor whereas the static model decomposes it into a magnitude and width.

To summarize the absolute peak magnitudes, the widths, and the fiducial constants are consistent with a static universe.

Although photometric-redshift results can predict redshifts, in a static model this is not evidence for time dilation. The use of spectroscopic aging can predict light-curve widths. But in a static model this is not a prediction of redshift. Consequently both results are consistent with the static model.

In an unrelated analysis it has been shown the number distribution of the (SNLS) SNe with redshift agrees with the static model without needing evolution or other ad hoc inclusions.

Finally note that if the SNe observations are fully explained by a static model the concept of dark energy or any other hypothesis invoked to explain the “expansion” of the universe is unnecessary.

5.1 Conclusions

The most important conclusions for this paper are:

- The type Ia supernovae are consistent with a static universe.
- There is no dark energy in a static universe.
- The density of type Ia supernovae is independent of redshift.

An important conclusion from previous Curvature Cosmology investigations that is relevant here is

- Dark matter is not required in a static universe.

6 ACKNOWLEDGEMENTS

This research has made use of NASA’s Astrophysics Data System Bibliographic Services. The calculations have been done using Ubuntu Linux and the graphics have been done using the DISLIN plotting library provided by the Max-Planck-Institute in Lindau.

REFERENCES

- Barboza, E. M., & Alcaniz, J. S. 2008, *Physics Letters B*, 666, 415
- Bazin, G., Ruhlmann-Kleider, V., Palanque-Delabrouille, N., et al. 2011, *A&A*, 534, A43
- Betoule, M., Kessler, R., Guy, J., et al. 2014, *A&A*, 568, A22
- Blondin, S., Davis, T. M., Krisciunas, K., et al. 2008, *ApJ*, 682, 724
- Conley, A., Guy, J., Sullivan, M., et al. 2011, *ApJS*, 192, 1
- Crawford, D. F. 1987a, *Australian Journal of Physics*, 40, 459
- . 1987b, *Australian Journal of Physics*, 40, 449
- . 1991, *ApJ*, 377, 1
- . 1993, *ApJ*, 410, 488
- . 1995a, *ApJ*, 440, 466
- . 1995b, *ApJ*, 441, 488
- . 1999, *Australian Journal of Physics*, 52, 753
- . 2006, *Curvature Cosmology* (BrownWalker Press)
- . 2009 <http://arxiv.org/abs/0901.4169>
- . 2009 <http://arxiv.org/abs/1009.0953>
- Goldhaber, G. 1997, in *NATO ASIC Proc. 486: Thermonuclear Supernovae*, ed. P. Ruiz-Lapuente, R. Canal, & J. Isern, 777
- Goldhaber, G., Boyle, B., Bunclark, P., et al. 1996, *Nuclear Physics B Proceedings Supplements*, Vol. 51, 51, 123
- Goldhaber, G., Groom, D. E., Kim, A., et al. 2001, *ApJ*, 558, 359
- Goliath, M., Amanullah, R., Astier, P., Goobar, A., & Pain, R. 2001, *A&A*, 380, 6
- Goobar, A., & Leibundgut, B. 2011, *Annual Review of Nuclear and Particle Science*, 61, 251
- Guy, J., Astier, P., Baumont, S., et al. 2007, *A&A*, 466, 11
- Hogg, D. W. 1999, *ArXiv:astro-ph/9905116*
- Holtzman, J. A., Marriner, J., Kessler, R., et al. 2008, *AJ*, 136, 2306
- Howell, D. A., Sullivan, M., Conley, A., & Carlberg, R. 2007, *ApJ*, 667, L37
- Kessler, R., Becker, A. C., Cinabro, D., et al. 2009, *ApJS*, 185, 32
- Leibundgut, B., Schommer, R., Phillips, M., et al. 1996, *ApJ*, 466, L21
- Mohlabeng, G. M., & Ralston, J. P. 2013, *ArXiv e-prints*
- Perlmutter, S., Aldering, G., Goldhaber, G., et al. 1999, *ApJ*, 517, 565
- Phillips, M. M. 1993, *ApJ*, 413, L105

- Riess, A. G., Strolger, L.-G., Casertano, S., et al. 2007, ApJ, 659, 98
- Sullivan, M., Guy, J., Conley, A., et al. 2011, ApJ, 737, 102
- Suzuki, N., Rubin, D., Lidman, C., et al. 2012, ApJ, 746, 85
- Tripp, R. 1998, A&A, 331, 815
- Wang, S., & Wang, Y. 2013, Phys. Rev. D, 88, 043511

APPENDIX A: STATIC COSMOLOGY

The static cosmology used here is Curvature Cosmology (Crawford 1987b,a, 1991, 1993, 1995a,b, 1999, 2006, 2009a,b) that is a complete cosmology that shows excellent agreement with all major cosmological observations without needing dark matter or dark energy. (Note that (Crawford 2009b) is an update with corrections of the previous work.) It is compatible with both (slightly modified) general relativity and quantum mechanics and obeys the perfect cosmological principle that the universe is statistically the same at all places and times. It was shown in those papers that all the major observations (except supernovae) which have been used as evidence of expansion are in fact consistent with a static model.

Curvature Cosmology is based on two major hypotheses. The first hypothesis is that the Hubble redshift is due to curvature redshift, which is due to an interaction of photons with curved spacetime where they lose energy to other very low energy photons. Thus it is a tired-light model. The basic premise is that the local quantum field describing a photon is propagated along geodesics and is therefore subject to the focussing theorem. The angular momentum is determined by a volume integral over the quantum field and if its transverse size is changed there is a change in angular momentum which is contrary to its fixed angular momentum. The resolution of this contradiction is that the photon decays into one photon with nearly all the energy and two very low energy photons. Because of symmetry the large energy photon maintains the same trajectory as the original photon. Thus there is no angular deviation that would produce fuzzy images of distant objects. The second hypothesis is that there is a reaction pressure (curvature pressure) acting on the material causing spacetime curvature from the acceleration of high velocity particles in curved spacetime. Since the acceleration of the particles is normal to their velocity there is no change in their energy. The major effect of curvature pressure is to provide stability in the cosmological model. The basic cosmology is for a simple universal model of a uniform high temperature plasma (cosmic gas) at a constant density.

The theory has a good fit to the background X-ray radiation between the energies of 10–300 keV. The fitted temperature was $2.62 \pm 0.04 \times 10^9$ K and the fitted density was equivalent to $N = 1.55 \pm 0.01$ hydrogen atoms per cubic meter (2.57×10^{-27} kg m⁻³). For the simple homogeneous model this density is the only free parameter in the theory of curvature cosmology. The observations recorded in the cited references show that curvature cosmology is consistent with the observations of: Tolman surface brightness, angular size, SNe (superseded by this paper), gamma ray bursts, galaxy luminosity distributions, quasar luminosity distributions, X-ray background radiation, cosmic microwave background radiation, quasar variability, radio source counts, and the Butcher–Oemler effect.

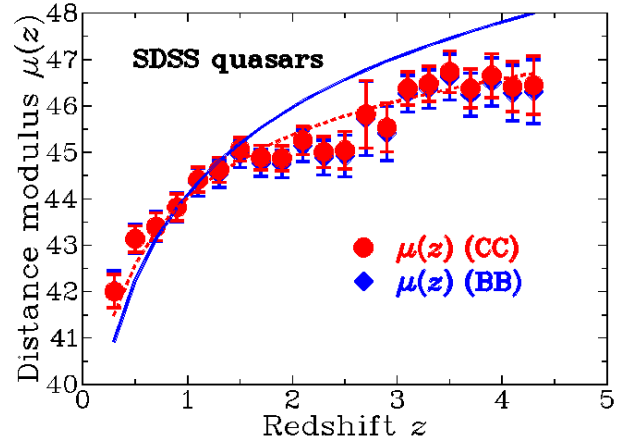


Figure A1. Plot of the distance modulus for SDSS quasars as a function of redshift, z . The solid (blue) line and blue triangles are for concordance cosmology. The dashed (red) line and red circles are for Curvature Cosmology. This figure is taken from (Crawford 2009a) (Figure 4). The difference between the blue and red data points is due to differential volume effects. Both theoretical curves were normalized to be equal to the data point at $z=0.9$. Clearly Curvature Cosmology provides a good fit to the observations.

In curvature cosmology the cosmic background radiation (CMB) is produced by the interaction of high energy electrons in the cosmic plasma with curved spacetime. The predicted temperature of the CMB is 3.18K to be compared with an observed value of 2.725K. The prediction does depend on the nuclei mix in the cosmic gas and could vary from this value by several tenths of a degree. It is argued that its black body spectrum arises from the large number of curvature redshift interactions undergone by the CMB photons.

In curvature cosmology the effect of a nearby high density low temperature (compared to 2.62×10^9 K) cloud is to increase the energy loss of the CMB due to curvature redshift without contributing new photons. For the Coma cluster the velocity dispersion of about 500 km s⁻¹ will produce a fractional decrease of about 0.004 in the CMB temperature. This contribution from many clouds may explain some of the CMB power spectrum.

As discussed in (Crawford 2009a) the quasar luminosity function is close to a power law in luminosity which is equivalent to an exponential distribution in magnitude. Consequently it is possible to estimate the two constants of the luminosity function for a group of quasars that have almost the same redshift. An estimate of the average apparent peak magnitude can be derived from these constants and it can be used as a “standard candle”. Assuming that luminosity function is the same at all redshifts these results can be used to estimate the distance modulus. The result is shown in Fig 5. Clearly Curvature Cosmology (CC) provides a good fit to the observations whereas the concordance results (BB) require inclusion of an evolutionary function.

Curvature redshift can explain the velocity dispersion of galaxies in the Coma cluster without requiring dark energy. Finally the anomalous acceleration of Pioneer 10 is explained by the effects of curvature redshift due to inter-planetary

dust producing a very small decrease in the radio frequencies sent to and from the spacecraft.

An important result of curvature redshift is that the rate of energy loss by a photon (to extremely low energy secondary photons) as a function of distance, ds , is given by

$$\frac{1}{E} \frac{dE}{ds} = - \left(\frac{8\pi G N M_H}{c^2} \right)^{\frac{1}{2}}, \quad (\text{A1})$$

where M_H is the mass of a hydrogen atom and the density in hydrogen atoms per cubic metrae is $N = \rho/M_H$. Equation (A1) shows that the energy loss is proportional to the integral of the square root of the density along the photon's path. The Hubble constant is predicted to be

$$\begin{aligned} H &= - \frac{c}{E} \frac{dE}{ds} = (8\pi G M_H N)^{\frac{1}{2}} \\ &= 51.69 N^{\frac{1}{2}} \text{ km s}^{-1} \text{ Mpc}^{-1} \\ &= 64.4 \pm 0.2 \text{ km s}^{-1} \text{ Mpc}^{-1} \quad (N = 1.55 \pm 0.01 \text{ m}^{-3}). \end{aligned} \quad (\text{A2})$$

The geometry is that of a three dimensional surface of a four dimensional hyper sphere. For this geometry the area of a three dimensional sphere with radius, $r = R\chi$ where $\chi = \ln(1+z)/\sqrt{3}$ (work prior to 2009 has $\chi = \ln(1+z)/\sqrt{2}$), is given by

$$A(r) = 4\pi R^2 \sin^2(\chi). \quad (\text{A3})$$

The surface is finite and χ can vary from 0 to π . The total volume v , is given by

$$\begin{aligned} v_C(r) &= 2\pi R^3 \left[\chi - \frac{1}{2} \sin(2\chi) \right] \approx \frac{4\pi}{3} (R\chi)^3 \\ &= \frac{32.648}{h^3} \left[\chi - \frac{1}{2} \sin(2\chi) \right] \text{ kpc}^3. \end{aligned} \quad (\text{A4})$$

The only other result required here is the equation for the distance-modulus, ($\mu_C = m - M$), which is

$$\mu_C = 5 \log \left[\frac{\sqrt{3} \sin(\chi)}{h} \right] + 2.5 \log(1+z) + 42.384 \quad (\text{A5})$$

where $h = H/100 \text{ km s}^{-1} \text{ Mpc}^{-1}$.

APPENDIX B: EXPANSION MODEL FUNCTIONS

The equations needed for the modified Λ -CDM model (Hogg 1999; Goliath et al. 2001; Barboza & Alcaniz 2008), with $\Omega_M = 0.27$, $\Omega_K = 0$ and where h is the reduced Hubble constant, are listed below. The symbol w^* is used for the acceleration parameter in order to avoid confusion with the width, w . These equations depend on the function $E(z)$ defined here by

$$E(z) = \int_0^z \frac{dz}{\sqrt{\Omega_M(1+z)^3 + (1-\Omega_M)(1+z)^{(1+w^*)}}}. \quad (\text{B1})$$

The distance modulus is

$$\mu_B(z) = 5 \log(E(z)(1+z)/h) + 42.384. \quad (\text{B2})$$

The co-moving volume is

$$v_B(z) = \frac{4\pi}{3} (2.998 E(z)/h)^3 \text{ Gpc}^3. \quad (\text{B3})$$

The equation of state parameter w^* in the expansion

model distance modulus is included to investigate the effects of including the cosmological constant. Conley et al. (2011) found that the parameter, w^* , has a value $w^* = -0.91$, whereas Sullivan et al. (2011) found that $w^* = -1.069$. Although its actual value is not critical for this paper the value of w^* is chosen to be $w^* = -1.11$, so that E_B would be the best fiducial constant with the values for the peak magnitudes and stretch factors provided by B14.

This paper has been typeset from a $\text{\TeX}/\text{\LaTeX}$ file prepared by the author.